Experimental verification of underwater positioning system in aquaculture

Stian Skaalvik Sandøy
Norwegian Univeristy of Science and Technology
Department of Marine Technology
Trondheim 7052, Otto Nielsensvei 10
Email: stian.s.sandoy@ntnu.no

Ingrid Schjølberg
Norwegian Univeristy of Science and Technology
Department of Marine Technology
Trondheim 7052, Otto Nielsensvei 10
Email: ingrid.schjolberg@ntnu.no

***Abstract*—This paper presents a filter for positioning of an underwater vehicle in exposed aquaculture environments. The input to the filter is time of flight measurements from acoustic transponders mounted at near the sea surface. The transponders are exposed to oscillations from wave disturbances. This has an impact on the accuracy of the positioning system. An extended Kalman filter (EKF) solution has been proposed with a wave motion compensation. Experimental results show that the proposed filter compensates for the disturbances and thereby increase performance of the position estimate.**

I. Introduction

A. Background and Motivation

There is a strong need for increasing global sea food production as the world population is growing significantly. Due to environmental challenges of local sea production there is a need to investigate the possibilities for more exposed aquaculture [1]. Remoteness and harsher environments motivate the use of Underwater Vehicles (UV) in inspection, maintenance, and repair (IMR) operations. Positioning and localization are key technologies for enabling such operations [2]. In the aquaculture industry, the overall goal is to reduce on-site manual operations for increased safety and reduced risk for workers [3], as well as to keep the cost of installation, operation and maintenance low. One way of doing this is increased use of remote operations and UVs. For efficient UV operations, there is a need for an underwater positioning system. Acoustic based technologies like long baseline (LBL), short baseline (SBL) and ultrashort baseline (USBL) systems are available for under water position. LBL systems use the same principle as Global Navigation Satellite Systems (GNSS). A receiver measures the time of flight (TOF) to multiple transponders and obtains a so called pseudo-range measurement. In the presented work transponders are mounted on the net pen to perform a long baseline network. The main focus of the presented work is to analyze and reduce the effect the disturbance of wave motion has on the near surface mounted transponders. The motion is caused by environmental disturbances like currents or waves and can create large errors in the position estimate if not contracted. It is essential that this error is as small as possible to ensure an accurate positioning of the UVs.

B. Literature review

This paper builds on the work presented in [4]. In the prvious work a filter with wave motion comensation was developed and verified by simulations. This work is further extended by a error spectrum analysis including verfication by experiments. Surveys on underwater navigation ([5]-[6]) discuss the sensors available, accuracy and how state estimation can be applied to fuse sensor information both for translation and attitude observers. A celebrated nonlinear filter for the latter is the complementary filter from [7] and later enhanced in [8]. A widely used extended Kalman filter (EKF) approach is presented in [9], also for attitude estimation. Furthermore, various translation observers using Kalman filter (KF) approaches are discussed in literature like [10]. Examples are Unscented KF, Ensemble KF and particle filter. However, in general, the nonlinear KF's are not proven globally stable in estimating position by pseudo ranges. Recently there has been a suggestion to transform the problem into a quasi-linear. The transformation was first suggested in [11]. Use for KF was first developed in [12], which made the implemented observer Global Exponential Stable (GES), but the transformation is optimal with noisy measurements. This can be resolved by using the Exogenous KF (XKF) presented in [13]. The KF using the quasi-linear model is here used as a linearization point for the next KF inheriting the stability properties and the noise reduction. A complete implementation for navigation using pseudo-range measurements is presented in [14]. Later, it has been implemented in combination with attitude filter in [15] using the attitude filter from [8]. Study of wave motions and sea states has been a wide research field. Examples can be found in [16], [17], [18].

C. Main Contribution

The main contribution of this paper is the experimental verification of the work presented in [4], where an error model was suggested. This is an important contribution since it enables mounting of transponders near the ocean surface on aquaculture structures in harsh conditions, without more expensive solutions like calculating the transponder position with GNSS in real time. The work solves the challenge

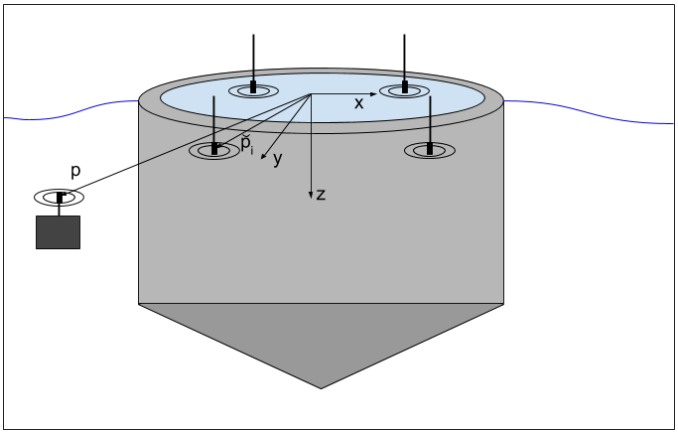

Fig. 1: Transponder configuration [4]

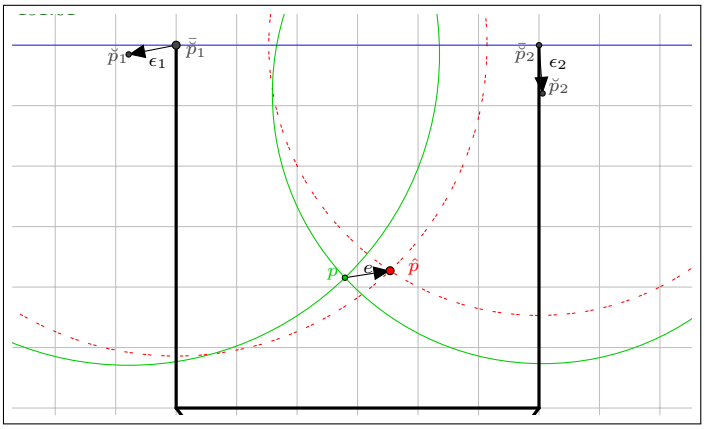

Fig. 2: Graphical position estimate $\hat{p}$ and solution p

of modeling the position estimate error. This error occurs because of the wave motion of the transponders. Moreover, the frequency spectra of the error is identified.

D. Notation

$(\cdot)^T$ is the transposed of a vector or matrix, and $||\cdot||$ is used as the euclidean norm. The set of real numbers are noted as $\mathbf{R}^{n\times m}$ with the dimension $n \times m$, where no indication $\mathbf{R}$ implies $m = 1$ and $n = 1$. $0_{p\times q}$ and $I_{p\times q}$ are the zero and identity matrix respectively, with dimension $p \times q$. Position will always be denoted as a vector $p = \begin{bmatrix} x & y & z \end{bmatrix}^T \in \mathbf{R}^{3\times 1}$ where x is surge, y is sway and z is heave. Wave motion vector will be designated $p_w = \begin{bmatrix} x_w & y_w & z_w \end{bmatrix}^T \in \mathbf{R}^{3\times 1}$. $N(0, \sigma^2)$ is a Normal Gaussian distribution with variance σ^2 and mean zero. $\hat{(\cdot)}$ is the notation for an estimated variable and $\bar{(\cdot)}$ denote an averaged value. For a matrix A and value x_i, $A = diag(x_1, \ldots, x_n) \in \mathbf{R^{n\times n}}$ means a matrix with diagonal terms x_1 to x_n and zeros everywhere else. For a function $h(x)$ and vector x, $\frac{\partial h(x)}{\partial x}$ is the notation for the partial derivative.

II. Problem Statement

The problem of oscillating transponders will be studied in an aquaculture environment around a net pen as seen in Figure 1. The transponders are mounted near the ocean surface in a non-rigid manner, meaning that wave disturbances should be considered. It can for instance be on the end of a flexible wire mounted at the surface. Two filter design cases are discussed in this paper. The former is denoted as A, and wave disturbances are not considered. In the latter case denoted as B, the wave disturbances are considered and contracted. The following section presents these and their assumptions. It should also be mentioned that the reference frame has an origin in the fish cage center at the mean sea surface. Positive z-axis points towards the sea floor and x-axis north. The y-axis complete the right hand rule, therefore pointing east. This is known as the North-East-Down (NED) reference frame [18]. The transponders and receiver position are denoted as $\breve{p}_i(t)$ with $i = 1, .., 4$ and p. Remark that in this work, the receiver position does not depend on time and is therefore static.

III. Mathematical Modeling

This section discusses of the mathematical model as presented in [4].

A. Pseudo-range Models

Figure 2 is a central illustration to understand the problem. Since waves are periodical it can be assumed that the influenced transponder positions will behave in a similar manner. Therefore, will this work simplify the problem to only consider the mean transponder position over a wave period denoted $\bar{\breve{p}}_i$. The difference for the real transponder position and average are denoted by ϵ_i. The mean and real transponder positions are encircled by a solid green and dotted red circle, respectively. Both circles have the same radius, which is $||p - \breve{p}_i||$ and consequently the intersection of the green circles is in point p. The red dotted circles centered at $\bar{\breve{p}}_i$ intersect in another point denoted $\hat{p}$, which is the estimated position if the position error e is not contracted. The next two points suggest two pseudo-range models denoted case A and B as suggested in the previous section.

Case A: Position error not considered

The following Equation use the estimated position $\hat{p}$.

$$y_i = (||\hat{p} - (\bar{\breve{p}}_i)|| + \epsilon_y) = h_i(x) \tag{1}$$

Measurement noise for each transponder is written as $\epsilon_y \in \mathbf{R}$ in $N(0, \sigma_m^2)$.

Case B: Position error considered

The measurement model considering position error is obtained inserting $\hat{p} = p + e$ as the following:

$$y_i = ||p + e - \bar{\breve{p}}_i|| + \epsilon_y = h_i(x) \tag{2}$$

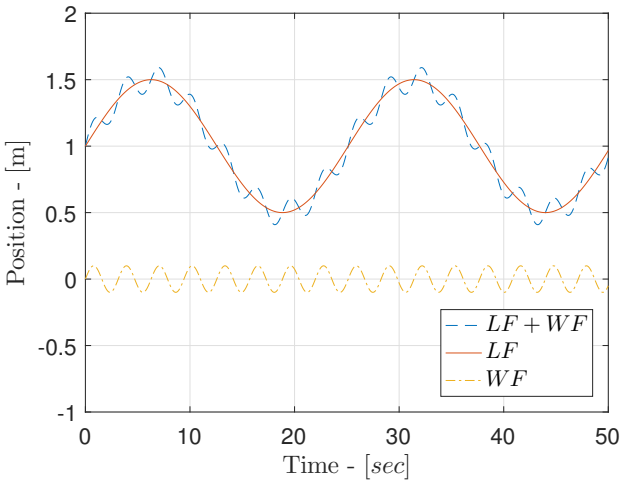

Fig. 3: Low (LF) and wave frequency (WF) motions [18].

B. Error Dynamics

To model the motion of the error we need to exploit that it will move in a wave motion pattern. This is why the second order wave model approximation is attractive. The goal of the wave motion model presented in this section is to separate the low and wave frequency motions. This is illustrated in Figure 3. The blue dashed line is the combined low and wave frequencies, while the red solid and yellow dash-dot line are the separated low and wave frequency motions, respectively. Here is the second-order wave model used for the separation of p and e given in Equation (2). This model originated in [17] and can also be found in newer literature [18]. The model is given as following:

$$\begin{bmatrix} \dot{\zeta} \\ \dot{e} \end{bmatrix} = A_w \begin{bmatrix} \zeta \\ e \end{bmatrix} + E_w \epsilon_w \in \mathbf{R}^{6\times 1} \tag{3}$$

where $\epsilon_w \in \mathbf{R}^{3\times 1}$ and each noise term is $N(0,1)$. Further, the matrices are defined as the following:

$$A_w = \begin{bmatrix} 0_{3\times 3} & I_{3\times 3} \\ -\omega_0^2 I_{3\times 3} & -2\lambda\omega_0 I_{3\times 3} \end{bmatrix}, E_w = \begin{bmatrix} 0_{3\times 3} \\ K_w \end{bmatrix}$$

where $K_w = diag(\sigma_{w1}, \sigma_{w2}, \sigma_{w3}) \in \mathbf{R}^{3\times 3}$.

C. Position Dynamics

A kinematic model is required in order to model the motion real position p. The velocity will be modeled as a random walk as following:

$$\dot{p} = A_p p + \epsilon_p \tag{4}$$

Where $\epsilon_p \in \mathbf{R}^{3\times 1}$ is $N(0, \sigma_p^2)$ and $A_p = 0_{3\times 3}$. Random walk is used because this case study only takes into account pseudo-range measurements. The velocity is not estimated in the work. It should be remarked that it is simple to also include a velocity state by including accelerometer measurements directly in the process model [14]. This would also improve the position estimates, of course depending on the quality of the accelerometer. However, since this is not the purpose of this paper, it is not taken into account. Only having position estimates also make it possible to further include this in a loosely coupled observer [19].

IV. Error Spectrum Analysis

This section discusses how to obtain the parameters for the position error dynamics model discussed in Section III-B. It is first necessary to derive a solution for the error e as seen in Figure 2. The error depends on the mean transponder $\bar{\breve{p}}$, transponder position error ϵ_i, and the real position p. In the next section we derived an algebraic solution for the error.

A. Algebraic Solution of the Error

Inspired by [11] and later used in ([14],[20],[21]) it is possible to find an exact solution of the error. Starting with one exact pseudo-range distance from Equation (5) using the time varying transponder position $\breve{p}(t)$. Equation (6) uses the mean position time invariant transponder position $\bar{\breve{p}}$ which will give an estimated position $\hat{p}$. ρ is the pseudo-range from the real transponder position to the real position as illustrated in in Figure 2 by the radius of the circles. Furthermore, we define an error trajectory of the transponder $\epsilon(t)$ such that $\breve{p}(t) =: \bar{\breve{p}} + \epsilon(t)$.

$$\rho^2 = ||p - \breve{p}_i(t)||^2 \tag{5}$$
$$\rho^2 = ||\hat{p} - \bar{\breve{p}}_i||^2 \tag{6}$$

Inserting this into Equation (5) results in the following:

$$\rho^2 = ||p - \bar{\breve{p}}_i||^2 + 2(\bar{\breve{p}}_i - p)^T \epsilon_i(t) + ||\epsilon_i(t)||^2 \tag{7}$$

From Equation (6) we can insert $\hat{p} =: p + e$ and obtain:

$$\rho^2 = ||p - \bar{\breve{p}}_i||^2 - 2(\bar{\breve{p}}_i - p)^T e + ||e||^2 \tag{8}$$

By further subtracting Equation (7) from (8) results in the following:

$$\underbrace{-2(\bar{\breve{p}}_i - p)^T}_{C_i} e + \underbrace{||e||^2}_{r} = \underbrace{2(\bar{\breve{p}}_i - p)^T \epsilon_i(t) + ||\epsilon_i(t)||^2}_{k_i} \tag{9}$$

Provided that we have $m \geq 3$ transponders and their positions $\breve{p}_i(t) = \bar{\breve{p}}_i + \epsilon(t)$, we can find the error trajectory $e(t)$ from Equation (9) by the following:

$$C = \begin{bmatrix} C_1 \\ \vdots \\ C_m \end{bmatrix}, \quad k = \begin{bmatrix} k_1 \\ \vdots \\ k_m \end{bmatrix} \tag{10}$$

Gathering all equations in matrix form as stated we obtain the following:

$$Ce + rl = k \tag{11}$$

Solving for e we obtain,

$$e = \underbrace{C^{-1}k}_{w} - r\underbrace{C^{-1}l}_{c} \tag{12}$$

Reformulating the variables as suggested Equation (12) and inserting this into $r = e^T e$ and solving for r we obtain the second order solution:

$$r = \begin{cases} \frac{-h \pm \sqrt{h^2 - w^T w c^T c}}{c^T c}, & if c^T c \neq 0 \\ -\frac{w^T M w}{2h}, & otherwise \end{cases} \tag{13}$$

where $h = 2c^T w - 1$. When r is obtained we can insert it into Equation (12) and obtain the difference between the real and estimated value. Figure 2 illustrates the computed solution e as a vector from p to $\hat{p}$ in two dimensions. The green circles are centered in the real varying transponder position with the radius of the distance between the real transponder position $\breve{p}$ and the red circles have centers in the averaged transponder positions and intersect to create the estimated solution $\hat{p}$. Further, the error between the estimated and real positions is denoted as the vector labeled e.

B. Position Error Spectrum

Using the error solutions of a given position we can obtain the error spectrum by obtaining a time serie of the transponder positions when induced by waves. This can then be used to approximate the parameters in the second order wave model given in Equation (3). The procedure can be summarized as the following:

1) Gather a time series of position of each transponder $\breve{p}_i(t)$ during wave disturbances.
2) Compute mean transponder positions $\bar{\breve{p}}_i$ and transponder errors ϵ_i
3) Compute the position errors e from Equation (12) and (13) given a position p.
4) Extract the error spectrum by using our favorite spectrum analysis tool for each degree of freedom. An example of a spectrum analysis tool is [22].
5) Fit the second order wave model in Equation (3) to the obtained error spectrum to identify the parameters ω_0, λ and σ^2 for each degree of freedom. A good fitting tool for this purpose is [23].

V. Extended Kalman Filter's Design

The general structure of the EKF for pseudo-range measurements is described in Figure 4 [10]. The filter estimate feedback $\bar{x}_k$, generates a linearized measurement matrix called C_k. Initially in the first iteration $k = 0$, and a guess $\bar{x}_0$ is used. The process and measurement equations will in this section be put together to fit the cases. Discrete process model will be defined as following:

$$\dot{x}_k = Ax_{k-1} + D\epsilon_k \tag{14}$$

where x_k is the state vector, A is the transition matrix, D is the noise driver matrix and ϵ_k is the noise vector with uncorrelated white noise terms which is $N(0, \sigma^2)$.

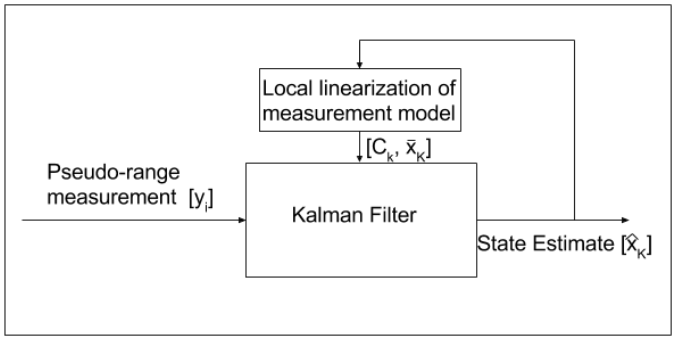

Fig. 4: General structure of EKF [24].

The state and noise vectors are defined as following:

$$x = \begin{bmatrix} \zeta \\ e \\ p \end{bmatrix}, \epsilon_k = \begin{bmatrix} \epsilon_w \\ \epsilon_p \end{bmatrix}$$

By using the state and noise vectors it is easy to find the A and D matrices followed by discretization to obtain Equation (14) by using Equation (4) and (3).

For the EKF it is also necessary to have a measurement matrix C_k. This is found by taking the Jacobian of Equation (2) . This is defined as following:

$$C_k = \frac{\partial h(x)}{\partial x} = \begin{bmatrix} C_{k,1} \\ \vdots \\ C_{k,m} \end{bmatrix} \in \mathbf{R}^{m \times 10}$$

where m is the number of pseudo-range measurements. The calculations result in the following:

$$\begin{aligned} C_{k,i} &= \frac{\partial h_i(x)}{\partial x}\Big|_{\bar{x}} \\ &= \begin{bmatrix} \frac{\partial h_i}{\partial \zeta} & \frac{\partial h_i}{\partial e} & \frac{\partial h_i}{\partial p} \end{bmatrix}\Big|_{\bar{x}} \end{aligned}$$

Where

$$\begin{aligned} \frac{\partial h_i}{\partial \zeta}\Big|_{\bar{x}} &= 0_{1\times 3} \\ \frac{\partial h_i}{\partial e}\Big|_{\bar{x}} = \frac{\partial h_i}{\partial p}\Big|_{\bar{x}} &= \frac{p + e - \bar{\breve{p}}_i}{||p + e - \bar{\breve{p}}_i||}\Big|_{\bar{x}} \end{aligned}$$

Now that both process and measurement model are derived, can the EKF be stated. The equations are as following [25]:

$$\begin{aligned} K_k &= \bar{P}_k C_k^T (C_k \bar{P} C_k^T + R_k)^{-1} \\ \hat{x}_k &= \bar{x}_k + K_k(y_k - h(\bar{x}_k))) \\ P_k &= (I_{n\times n} - K_k C_k)\bar{P}_k \\ \bar{x}_k &= A\hat{x}_{k-1} \\ \bar{P}_k &= AP_{k-1}A^T + Q_d \end{aligned}$$

where $Q_d \in \mathbf{R}^{n\times n}$ and $R \in \mathbf{R}^{m\times m}$ are the process and sensor noise covariance matrices, respectively. Furthermore,

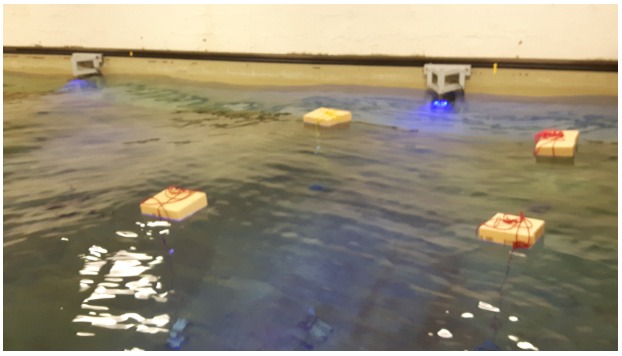

Fig. 5: Experimental setup in the marine cybernetics lab

n and m correspond respectively to the number of states and measurements. P_k is the covariance matrix. Note that $(\bar{\cdot})$ marks posterior estimates. Also, it should be noted that in the first iteration, $k = 0$, the initial values $\bar{x}_0$ and $\bar{P}_0$ are used. Remark that the EKF design is only modeled for case B. For case A we use the exact algebraic solution such that $\hat{p} = p + e$.

VI. Experimental Setup

An experimental setup to test the EKF design was performed in the Marine Cybernetics Lab at NTNU Norwegian University of Science and technology. Four Qulisys markers [26] were placed under the water surface supported by wires, which were mounted at buoyancy elements. They were oscillated by regular waves generated by a wave maker. An image of the setup is shown in Figure 5.

In this case the wave frequency was set to $\omega = 3.5863$, which gave a wave length of $L = 4.6$ and the wave hight was 0.05 m. This was approximately twice the length between transponder positions in the wave direction in calm water. Firstly, it was necessary to identify the parameters in Equation (3) in order to model the error. This was performed by following the procedure in Section IV-A. The transponder positions were captured by Qualisys Motion System [26] while induced by waves for 300 seconds with a time step of 0.02 second. The logged data determined the mean transponder positions $\bar{\bar{p}}_i$ and ϵ_i. The mean transponder positions and real position are the following:

$$\bar{\bar{p}}_1 = \begin{bmatrix} -0.28 & 0.35 & 0.46 \end{bmatrix}^T, \quad \bar{\bar{p}}_2 = \begin{bmatrix} 1.77 & 0.25 & 1.44 \end{bmatrix}^T$$
$$\bar{\bar{p}}_3 = \begin{bmatrix} 2.09 & -1.79 & 2.15 \end{bmatrix}^T, \quad \bar{\bar{p}}_4 = \begin{bmatrix} 0.09 & -1.81 & 4.14 \end{bmatrix}^T$$
$$p = \begin{bmatrix} -1.82 & -0.81 & 0.28 \end{bmatrix}^T$$

Further, the error spectrum was computed and the error dynamics in Equation (3) was fitted and both plotted in Figure 6

Axis	ω_0	λ	σ
x	3.59	2.9e-3	1.07
y	3.59	2.9e-3	0.94
z	3.59	2.8e-3	1.35

TABLE I: Parameters for error model

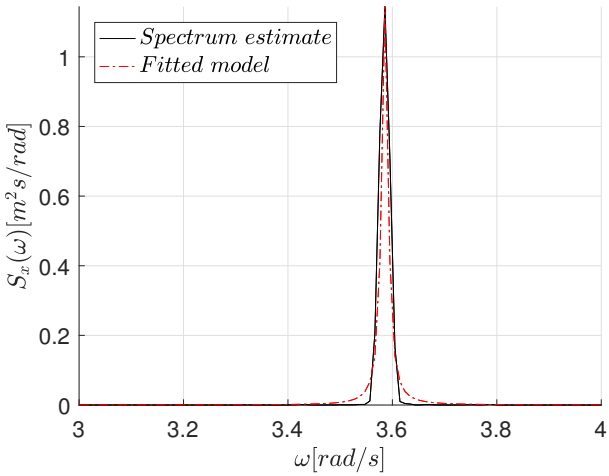

Fig. 6: Estimted and fitted spectrum for position error e in x-direction.

for the error in x-direction. The black solid line is the spectrum estimate and the red dashed line is the model fit of Equation (3). The resulting parameters are presented in Table I. These parameters are implemented with the EKF design from Section V using Matlab. The filter is tested by using the same 300 second long time series as used for the parameter estimation. Note that the positions were converted into pseudo-ranges by using Equation (5) before running it through the EKF implementation. The initial states in the EKF were set to $\bar{x}_0 = \begin{bmatrix} 0_{9\times1} \end{bmatrix}$. The sensor noise covariance matrix $R = diag(\sigma_m^2, \sigma_m^2, \sigma_m^2, \sigma_m^2)$, where $\sigma_m^2 = 0.1$. Process noise covariance matrix is set to $Q = diag(1_{1\times3}, \sigma_p^2, \sigma_p^2, \sigma_p^2) \in \mathbf{R}^{6\times6}$, where $\sigma_p^2 = 0.1$. The discretized process noise denoted by Q_d is approximated by Taylor expansion a as suggested in [24]. The initial covariance matrix is set to $P_0 = diag(1_{1\times3}, \omega_0 1_{1\times3}, 1_{1\times3}) \in \mathbf{R}^{9\times9}$, where the subscripts denote dimensions. The filter's update rate is set to 50 Hz, which is the same as the measurement frequency.

VII. Results and Discussions

The experimental results are presented in Table II and Figure 8-7. Figure 7 presents EKF estimated positions against the real position p and the uncompensated position $\hat{p}$ as well as the EKF estimated errors e along with the real ones form the algebraic solution. Figure 7a shows the combination of real low and wave frequency motions, $\hat{x}$, shown by a solid blue line. Furthermore, it shows the EKF estimated real position drawn as a red dashed line and the real position x in a black solid line. From these, we can see that the estimate converges to the real position at $x = -1.82$, as defined in Section VI. Figure 7c shows that the same occurs in heave direction. Note that the waves are not oscillating the markers before approximately 25 seconds into the time series. Figure 7b and 7d show a 20 second plot of the estimated error $\hat{e}$ in a red dashed line against the real error e in a black solid line from 200 to 220 seconds. They show that the estimation is correct. However, since the error is not oscillating perfectly around

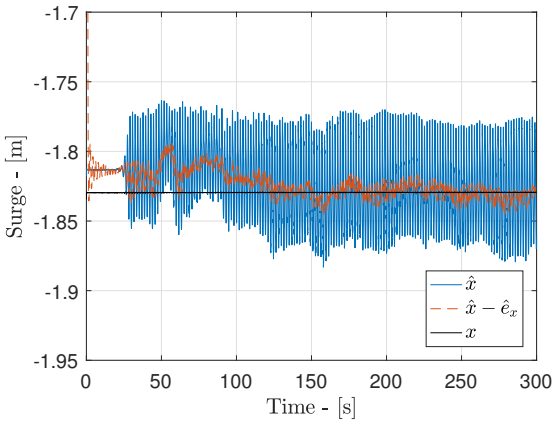

(a) Surge estimated position.

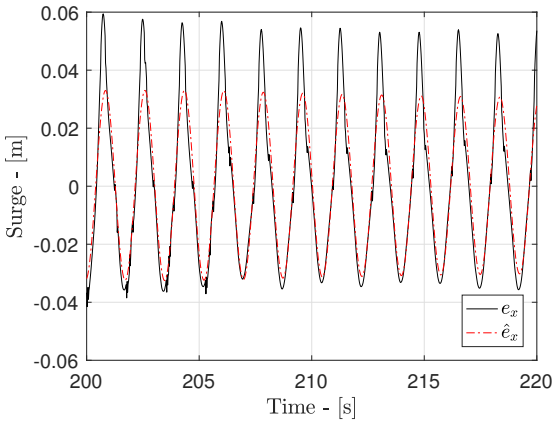

(b) Surge error estimated.

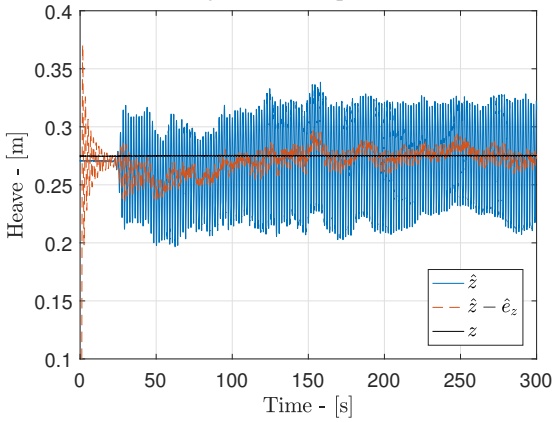

(c) Heave estimated position

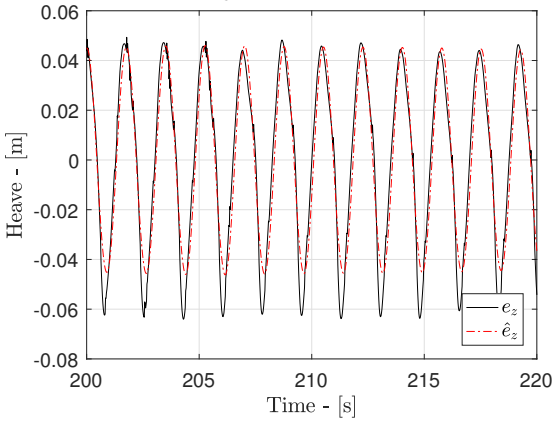

(d) Heave error estimated

Fig. 7: Estimated states with EKF

zero it is difficult for the error model to capture all motions, but it is a good approximation. Figure 8 shows how the covariance matrix converges towards steady state values. This effectively means that the filter converges. Table II compares the root mean square values for the converged filter against the position error e. It shows a considerable decrease from uncompensated to compensated. It is an reduction of almost 80% in x- and z-directions.

RMS	$x[m]$	$y[m]$	$z[m]$
Uncompensated	0.0292	0.0281	0.03366
Compensated	0.0062	0.0167	0.0076
Decrese in RMS	78.8%	40.5%	77.4%

TABLE II: RMS Error for case A and B

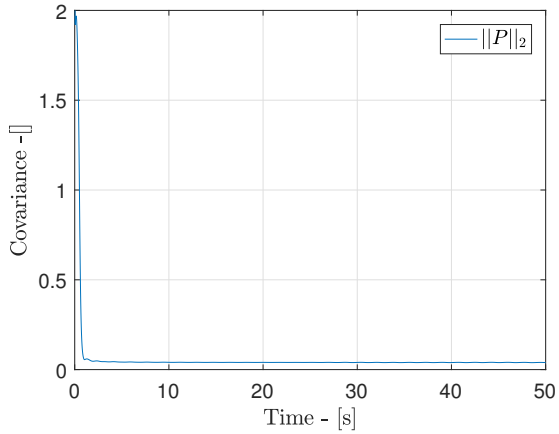

Fig. 8: Norm of the covariance matrix from the EKF ($||P||_2$)

VIII. Conclusion and Further Work

This paper presents an experimental verification of an EKF design building on [4]. Demanding weather conditions will impose oscillations on the transponders near the surface area. The work presents a method for identifying parameters for an error model. The final EKF design was experimentally tested in the Marine Cybernetics lab at NTNU. The results show that the EKF compensates for the wave motion resulting in a considerable decrease in RMS values in comparison to no compensation. Further work will consist in an experimental verification of the design in an aquaculture environment.

Acknowledgment

This work is funded by the Norwegian University of Science and Technology (NTNU), Norwegian Research Council

projects Reducing Risk in Aquaculture (254913) and SFI Exposed (237790).

REFERENCES

[1] H. V. Bjelland and et.al., "Exposed aquaculture in norway," in *OCEANS 2015 - MTS/IEEE Washington*, Conference Proceedings, pp. 1–10, 2015.

[2] I. Schjolberg, T. B. Gjersvik, A. A. Transeth, and I. B. Utne, "Next generation subsea inspection, maintenance and repair operations," *IFAC-PapersOnLine*, vol. 49, no. 23, pp. 434–439, 2016. [Online]. Available: http://www.sciencedirect.com/science/article/pii/S2405896316320316

[3] I. B. Utne, I. Schjolberg, and I. M. Holmen, "Reducing risk to aquaculture workers by autonomous systems and operations. i: Safety and reliability of complex engineered systems," 2015.

[4] S. Sandoy and I. Schjolberg, "Underwater positioning using near surface long baseline transponder's induced by wave motion," 2017, accepted for OMAE 2017.

[5] J. C. Kinsey, R. M. Eustice, and L. L. Whitcomb, "A survey of underwater vehicle navigation: Recent advances and new challenges," in *IFAC Conference of Manoeuvering and Control of Marine Craft*, vol. 88, Conference Proceedings, 2006.

[6] J. J. Leonard and A. Bahr, *Autonomous Underwater Vehicle Navigation*. Cham: Springer International Publishing, 2016, pp. 341–358.

[7] R. Mahony, T. Hamel, and J. M. Pflimlin, "Nonlinear complementary filters on the special orthogonal group," *IEEE Transactions on Automatic Control*, vol. 53, no. 5, pp. 1203–1218, 2008.

[8] H. F. Grip, T. I. Fossen, T. A. Johansen, and A. Saberi, "Globally exponentially stable attitude and gyro bias estimation with application to gnss/ins integration," *Automatica*, vol. 51, pp. 158–166, 2015.

[9] F. L. Markley, "Attitude error representations for kalman filtering," *Journal of Guidance, Control, and Dynamics*, vol. 26, no. 2, pp. 311–317, 2003.

[10] C.-T. Chen, *Linear system theory and design*, fourth edition. ed., ser. The Oxford series in electrical and computer engineering. New York: Oxford University Press, 2013.

[11] S. Bancroft, "An algebraic solution of the gps equations," *IEEE Transactions on Aerospace and Electronic Systems*, vol. AES-21, no. 1, pp. 56–59, 1985.

[12] P. Batista, "Ges long baseline navigation with unknown sound velocity and discrete-time range measurements," in *52nd IEEE Conference on Decision and Control*, Conference Proceedings, pp. 6176–6181, 2013.

[13] T. A. Johansen and T. I. Fossen, "The exogenous kalman filter (xkf)," *International Journal of Control*, pp. 1–7, 2016. [Online]. Available: http://dx.doi.org/10.1080/00207179.2016.1172390

[14] T. A. Johansen, T. I. Fossen, and G. C. Goodwin, "Three-stage filter for position estimation using pseudorange measurements," *IEEE Transactions on Aerospace and Electronic Systems*, vol. 52, no. 4, pp. 1631–1643, 2016.

[15] T. A. Johansen and T. I. Fossen, "Nonlinear observer for tightly coupled integration of pseudorange and inertial measurements," *IEEE Transactions on Control Systems Technology*, vol. 24, no. 6, pp. 2199–2206, 2016.

[16] O. M. Faltinsen, *Sea loads on ships and offshore structures*, ser. Cambridge ocean technology series. Cambridge: Cambridge University Press, 1990.

[17] J. G. Balchen, N. A. Jenssen, and S. Saelid, "Dynamic positioning using kalman filtering and optimal control theory," in *IFAC/IFIP symposium on automation in offshore oil field operation*, vol. 183, Conference Proceedings, p. 186, 1976.

[18] T. I. Fossen, *Handbook of Marine Craft Hydrodynamics and Motion Control*. Wiley, 2011.

[19] P. D. Groves, *Principles of GNSS, inertial, and multi-sensor integrated navigation systems*. Boston/ London: Artech House, 2008.

[20] B. B. Stovner, T. A. Johansen, T. I. Fossen, and I. Schjolberg, "Three-stage filter for position and velocity estimation from long baseline measurements with unknown wave speed," in *2016 American Control Conference (ACC)*, Conference Proceedings, pp. 4532–4538, 2016.

[21] E. K. Jorgensen, T. A. Johansen, and I. Schjolberg, "Enhanced hydroacoustic range robustness of three-stage position filter based on long baseline measurements with unknown wave speed*," *IFAC-PapersOnLine*, vol. 49, no. 23, pp. 61–67, 2016. [Online]. Available: http://www.sciencedirect.com/science/article/pii/S2405896316319097

[22] MathWorks, "pwelch," 20.04.2017 2017. [Online]. Available: https://se.mathworks.com/help/signal/ref/pwelch.html

[23] ——, "lsqcurvefit," 20.04.2017 2017. [Online]. Available: https://se.mathworks.com/help/optim/ug/lsqcurvefit.html

[24] J. Farrell, *Aided Navigation: GPS with High Rate Sensors*. McGraw-Hill Education, 2008. [Online]. Available: https://books.google.no/books?id=yNujEvIMszYC

[25] R. G. Brown and P. Y. C. Hwang, *Introduction to Random Signals and Applied Kalman Filtering with Matlab Exercises, 4th Edition*, ser. Introduction to random signals and applied Kalman filtering. John Wiley and Sons, 2012.

[26] Qualisys, "Oqus underwater - motion capture camera for advanced underwater measurements," 20.04.2017 2015. [Online]. Available: http://www.qualisys.com/cameras/oqus-underwater/